RESEARCH ARTICLE

Comparative proteomic analysis to discover potential therapeutic targets in human multiple myeloma

Chuan-Le Xiao[1], Zhi-Ping Zhang[2]*, Sheng Xiong[1], Chun-Hua Lu[1], Hong-Ping Wei[2], Hui-Lan Zeng[3], Zhi Liu[4], Xian-En Zhang[2]** and Feng Ge[1]*

[1] Institute of Life and Health Engineering, Jinan University, Guangzhou, P. R. China
[2] State Key Laboratory of Virology, Wuhan Institute of Virology, Chinese Academy of Sciences, Xiao Hong Shan, Wuhan, P. R. China
[3] Department of Hematology, the First Affiliated Hospital, Jinan University, Guangzhou, P. R. China
[4] Department of Hematology, Nanfang Hospital, Southern Medical University, Guangzhou, P. R. China

Received: April 12, 2009
Revised: June 17, 2009
Accepted: August 8, 2009

To clarify the molecular mechanisms that participate in the formation of multiple myeloma (MM) and to detect any tumor-related biomarkers, we performed proteomic analysis of cellular protein extracts from MM cells and normal plasma cells. Plasma cells from nine patients with newly diagnosed MM and nine healthy donors were purified by using anti-CD138 based immunomagnetic bead-positive selection. The protein profiles of purified MM and normal plasma cells were compared using 2-DE. We identified a total of 43 differentially expressed proteins, and confirmed with Western blotting six proteins. The altered proteins were analyzed using the software program Pathway Studio and the biological network can be accessed *via* (http://life-health.jnu.edu.cn/pathway/pathway.html). Further functional studies showed that annexin A1 knock down modestly induces lethality alone and potentiates the effects of dexamethasone on both dexamethasone-sensitive and dexamethasone-resistant MM cells. By correlating the proteomic data with these functional studies, the current results provide not only new insights into the pathogenesis of MM but also direct implications for the development of novel anti-MM therapeutic strategies and could lead to the discovery of potential therapeutic targets. Future molecular and functional studies would provide novel insights into the roles of these dysregulated proteins in the molecular etiology of MM.

Keywords:
Annexin A1 / Multiple myeloma / Plasma cell

1 Introduction

Multiple myeloma (MM) is a clonal B-cell disorder in which malignant plasma cells (PCs) expand and accumulate in the bone marrow (BM), leading to cytopenias, bone resorption, and the production (in most cases) of the characteristic monoclonal protein [1]. It is the second most common adult hematologic malignancy, and the most common cancer with skeleton as its primary site. It has an incidence of 19 900 new cases *per* year in the USA, and accounts for 10% of hematologic malignancies and 1% of all cancer deaths [2]. In China, the annual incidence of MM is approximately one case *per* 100 000 persons [3].

MM remains incurable, but recent advances in cytogenetic techniques and molecular profiling technologies have allowed for advances in our understanding of disease pathogenesis, identified novel therapeutic targets, allowed for molecular classification, and provided the scientific rationale for combining targeted therapies to increase tumor cell cytotoxicity and abrogate drug resistance [4]. The current focus on RNA in expres-

Correspondence: Dr. Feng Ge, Jinan University, Institute of Life and Health Engineering, Guangzhou 510632, P. R. China
E-mail: tgfeng@jnu.edu.cn
Fax: +86-20-8522-4372

Abbreviations: BM, bone marrow; **MM,** multiple myeloma; **NPC,** normal plasma cell; **PC,** plasma cell; **SLO,** Streptolysin-O

*These authors contributed equally to this work.
**Additional corresponding author: Dr. Xian-En Zhang, E-mail: x.zhang@wh.iov.cn

sion profiling has generated extensive datasets relating to MM, but ultimately protein expression and PTM determine MM formation. Thus, the molecular analysis of MM would greatly benefit from a proteomics approach that combines the advantages of high throughput analysis (as in expression profiling) and the focus on protein levels and modifications. Proteomics offers excellent possibilities for determining the array of proteins involved in the signalling pathways and regulatory biology of PCs. Moreover, proteomics permits to identify isoforms, co-translational modification and PTM of proteins, which underlie different stages of MM formation [5]. There were many reports that both normal and malignant PCs can be purified to homogeneity from BM aspirates using anti-CD138-based immunomagnetic bead-positive selection [6]. Thus, MM represent a good model for proteome research because they can be obtained as a pure cell population in high yield.

Proteomic techniques as a powerful research tool have recently become available for large-scale protein analysis and 2-D PAGE is one of the most effective methods for the simultaneous detection of diverse changes in protein expression and the high-resolution separation of proteins [7]. In recent years, different proteomic approaches have been performed investigating various aspects concerning MM [8]. Furthermore, proteomics has been a useful tool for identifying drug targets and therapeutic agents to treat MM [9, 10].

In the present study, using 2-DE coupled with anti-CD138-based immunomagnetic bead-positive selection, we compared protein expression profiles of MM and normal plasma cells (NPC), and identified differentially expressed proteins that might be crucial to the pathogenesis of MM. By correlating the proteomic data with further functional studies, the current results provide not only insights into the mechanism underlying MM formation but also direct implications for the development of novel anti-MM therapeutic strategies and could lead to the discovery of potential therapeutic targets.

2 Materials and methods

2.1 Cell lines and reagents

The human MM RPMI8226 and MM1.s cell line were cultured in RPMI 1640 supplemented with 1% penicillin/streptomycin, 1 mmol/L L-glutamine, and 10% FBS at 37°C, 5% CO_2 in air. Dexamethasone was purchased from Sigma (St. Louis, MO, USA). All other reagents were purchased from GE Healthcare (Uppsala, Sweden) unless otherwise stated.

2.2 Patient samples

BM aspirates were obtained from nine patients with newly diagnosed MM and nine healthy donors. Informed consent was obtained in accordance with the institutional policies and the Declaration of Helsinki protocol. Mononuclear cells

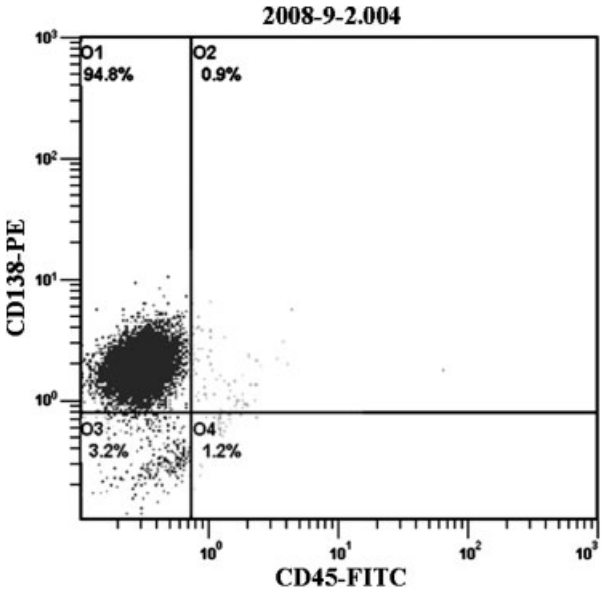

Figure 1. An example of flow cytometry report of CD138-enriched BM PCs. Antibodies used in individual FACS analyses are indicated to the left and bottom of each FACS plot. The percentage of cells in each gate window is indicated.

(including PCs) were isolated from BM biopsies by purification over a Ficoll-Paque (Amersham, Piscataway, NJ, USA) gradient centrifugation. Briefly, BM aspirates (approximately 15 mL) were diluted 1:1 with prewarmed (37°C) PBS and overlaid onto 15 mL prewarmed Ficoll-Hypaque. After centrifugation at 2000 rpm for 20 min at room temperature, mononuclear cells were removed, washed again with PBS. PC isolation from mononuclear cell fraction was performed by immunomagnetic bead selection with monoclonal mouse anti-human CD138 antibodies in association with LS separation columns separation system (Miltenyi Biotec, Bergisch Gladbach, Germany). The purity of the isolated PCs was monitored by BD-FACScalibur flow cytometry (BD Biosciences, San Jose, CA, USA) using $CD138^+/CD45^-$ and $CD38^+/CD45^-$ criteria [11]. PC purity of more than 95% homogeneity was confirmed (Fig. 1).

2.3 2-DE

Purified PCs were washed three times with ice-cold washing buffer (10 μM Tris-HCl, 250 μM sucrose, pH 7.0) and transferred to a clean 1.5 mL Eppendorf tube. Cells were lysed with a buffer containing 7 M urea, 2 M thiourea, 4% CHAPS, and 1% DTT, 2% v/v IPG buffer 3–10 NL, 0.2 mg/mL PMSF, and protease-inhibitors (Complete kit, Roche Diagnostics, Germany). Cellular debris was removed by centrifugation for 30 min at 13 200 × *g* and at 4°C. The lysis supernatant was used for 2-DE. Protein concentrations were determined using Bradford assay. All the samples were stored at −80°C before electrophoresis.

2-DE was performed with Amersham Biosciences IPGphor IEF System and Hoefer SE 600 (GE Healthcare) electrophoresis units using the protocol suggested by the manufacturer. Briefly, total proteins (110 μg) were mixed up to 250 μL of rehydration solution (8 M urea, 2% CHAPS, 20 mM DTT, and 0.5% IPG buffer) and run in IEF using a 13-cm immobilized pH 3–10 nonlinear gradient IPG strips. The rehydration step was carried out for 10 h at low voltage of 30 V. IEF was run following a step-wise voltage increase procedure: 500 and 1000 V for 1 h each and 5000–8000 V for about 10 h with a total of 64 kVh. After IEF, the strips were subjected to two-step equilibration in equilibration buffers (6 M urea, 30% glycerol, 2% SDS, and 50 mM Tris-HCl pH 6.8) with 1% DTT w/v for the first step, and 2.5% IAA (w/v) for the second step. The equilibrated gel strip was placed on top of a 12.5% SDS-PAGE gel and sealed with 0.5% agarose containing a little bromophenol blue. SDS-PAGE was performed for 30 min at a constant current of 15 mA *per* gel and then 30 mA *per* gel until the bromophenol blue reached the bottom of the gels. Proteins were detected by a silver nitrate staining.

2.4 Image analysis

Analytical gels were scanned on an Image Scanner (GE Healthcare) at 300 dpi with 12-bit gray scale levels in tagged image file format, and images were analyzed using the ImageMaster 2D Platinum (GE Healthcare). All gels in the analyses were scanned with identical parameters. To perform differential analysis of the 2-D gels with the ImageMaster 2D Platinum software, the individual spots of each gel were detected by their boundaries, and the spot volume corresponding to the protein abundance was calculated automatically. Each spot intensity volume was processed by background subtraction and total spot volume normalization; the resulting spot volume percentage was used for comparison. Manual editing of the gels was necessary especially in the higher molecular weight region. Proteins were classified as being differentially expressed between the two types of samples when spot intensity showed a difference of >2-fold variation in MM in comparison to NPC. The normalized value for each protein spot volume was used for comparison. One-tailed Student's *t*-test was used for statistically analyzing the data extracted from comparison window of ImageMaster software that displayed the normalized volumes for each protein spot. A value of $p<0.05$ was considered significant. Only those spots that have statistical significance in differential expression were excised from gels for analysis by MS.

2.5 Tryptic in-gel digestion and MALDI-TOF/TOF analysis

Protein spots were excised and transferred into siliconized 0.5 mL Eppendorf tubes. Each gel piece was rinsed twice with deionized water, destained in a 1:1 solution of 30 mM potassium ferricyanide and 100 mM sodium thiosulfate and then equilibrated in 50 mM ammonium bicarbonate to pH 8.0. After hydrating with ACN and drying in a Speed Vac (Thermo Fisher Scientific, Waltham, MA, USA), the gel spots were rehydrated in a minimal volume of trypsin (Promega, USA) solution (20 μg/mL in 25 mM NH_4HCO_3) and incubated at 37°C overnight. The supernatants were transferred into a 200 μL microcentrifuge tube and the gels were extracted once with extraction buffer (67% ACN containing 2.5% TFA). The peptide extract and the supernatant of the gel spot were combined and then completely dried in a SpeedVac centrifuge. Protein digestion extracts (tryptic peptides) were resuspended with 5 μL of 0.1% trifluoroacetic acid and then the peptide samples were mixed (1:1 ratio) with a matrix consisting of a saturated solution of CHCA in 50% ACN containing 0.1% TFA. Aliquots of 0.8 μL were spotted onto stainless steel sample target plates.

Peptide mass spectra were obtained on an ABI 4800 MALDI TOF/TOF mass spectrometer (Applied Biosystems, Foster City, CA, USA). All spectra were obtained using the settings presented in the Supporting Information Table 1. Data were acquired in positive MS reflector using a CalMix5 standard to calibrate the instrument (ABI4700 Calibration Mixture). Mass spectra were obtained from each sample spot by accumulation of 600–800 laser shots in an 800–4000 mass range. For MS/MS spectra, the five most abundant precursor ions *per* sample were selected for subsequent fragmentation and 900–1200 laser shots were accumulated *per* precursor ion. The criterion for precursor selection was a minimum S/N of 50. Both the MS and MS/MS data were interpreted and processed by using the GPS Explorer software (V3.6, Applied Biosystems), and then the obtained MS and MS/MS spectra *per* spot were combined and submitted to MASCOT search engine (V2.1, Matrix Science, London, UK) by GPS Explorer software and searched with the following parameters: IPI Human database (V3.36), taxonomy of Homo sapiens (human), trypsin of the digestion enzyme, one missed cleavage site, partial modification of cysteine carboamido methylated and methionine oxidized, none-fixed modifications, MS tolerance of 30–60 ppm, MS/MS tolerance of 0.2–0.3 Da. Known contaminant ions (keratin) were excluded. Total of 69 012 sequences and 29 002 682 residues in the database were actually searched. MASCOT protein scores (based on combined MS and MS/MS spectra) of greater than 65 were considered statistically significant ($p\leq0.05$). The individual MS/MS spectrum with statistically significant ($p\leq0.05$) best ion score (based on MS/MS spectra) was also accepted.

2.6 Protein categorization and network construction

Differentially expressed proteins were classified based on the PANTHER (Protein ANalysis THrough Evolutionary Relationships) system (http://www.pantherdb.org), which is

a unique resource that classifies genes and proteins by their functions [12]. In the process, the PANTHER ontology, a highly controlled vocabulary (ontology terms) by biological process, molecular function, and molecular pathway, was used to categorize proteins into families and subfamilies with shared functions. Some proteins were annotated manually based on literature searches and closely related homologues.

The differentially expressed protein interaction network was generated with Pathway Studio version 5.0 software (Ariadne Genomis, Rockville, MD, USA) and Resnet 5 [13] database were used. Common downstream targets or upstream regulators of multiple proteins were identified by using this software, which facilitated the process of selecting key factors and potential mechanisms from the large number of differentially regulated proteins.

2.7 Western blot analysis

Six proteins were selected for WB verification, which are profilin-1, glutathione peroxidase 1, annexin A1, proteasome subunit alpha type-5 (PSMA5), proteasome activator subunit 2 (PSME2), and proteasome subunit beta type-10 (PSMB10). PCs purified from six newly diagnosed MM patients and six healthy donors were used for Western blotting. Protein extracts (25 μg) prepared with RIPA lysis buffer (50 mM Tris-HCl, 150 mM NaCl, 0.1% SDS, 1% NP-40, 0.5% sodium deoxycholate, 1 mM PMSF, 100 mM leupeptin, and 2 mg/mL aprotinin, pH 8.0) were resolved by a 10% SDS-PAGE gel, and transferred onto a Immobilon-P PVDF transfer membrane (Millipore, Bedford, MA, USA) by electroblotting. After blocking with 5% nonfat milk, the membranes were probed with mouse anti-annexin A1 monoclonal, goat anti-profilin-1 polyclonal, goat anti-glutathione peroxidase 1 polyclonal antibody (Santa Cruz Biotechnology, Santa Cruz, CA, USA), mouse anti-PSMA5 monoclonal (Enzo Life Sciences, Germany), mouse anti-PSMB10 monoclonal, mouse anti-PSME2 monoclonal (Abcam, Cambridge, MA, USA), and mouse anti-tubulin monoclonal antibody (LabVision, Fremont, CA, USA). Blots were then incubated with peroxidase-conjugated anti-mouse or anti-goat IgG (KPL, Gaithersburg, MD, USA) for 1 h at room temperature at a 1:3000 dilution and then developed by using the SuperSignal West Pico kit (Pierce Biotechnology, Rockford, IL, USA).

2.8 siRNA for annexin A1 and transfection of siRNA

Annexin A1 RNA interference mediated by duplexes of 21-nucleotide RNA was performed in RPMI8226 or MM1.s cells. The siRNA duplex targeted against annexin A1 and the nonsilencing negative control siRNA duplex were purchased from Shanghai GenePharma (Shanghai, China). For initial screening of siRNAs, MM cells were transfected and the knockdown was estimated by using Western blotting. From this screen, Annexin A1 siRNA (5′-ACUCCAGCG-CAAUUUGAUGTT-3′) was chosen as the main siRNA with the most efficient knockdown. The RNA sequence used as a negative control for siRNA activity was: 5′-UUCUCCGAAC-GUGUCACGUTT-3′. All duplexes were dissolved in RNAse-free water to a final concentration of 20 μM. Dissolved siRNA duplexes were aliquoted and stored at −20°C.

In preliminary experiments, we optimized conditions for the efficient transfection using FAM-labeled negative control siRNA duplex. Streptolysin-O (SLO) (Sigma Chemical, Poole, England) was used to reversibly permeabilize cells toward siRNA according to a recently revised protocol [14]. Briefly, SLO was dissolved in RNAse-free water to 1000 U/mL and activated with 5 mM DTT for 2 h at 37°C, and then checked for activity and frozen in aliquots at −20°C until required. Cells for permeabilization were washed and resuspended at 10^7 cells *per* 400 μL in serum-free RPMI 1640. SLO (10 U/10^6 cells) was added in the presence or absence of 5 μmol/L siRNA and incubated at 37°C for 10 min, during which cells were mixed twice. The precise amounts of SLO required for optimal permeabilization and resealing were identified immediately prior to each experiment by a dose–response optimization procedure. Resealing was achieved by the addition of 1 mL prewarmed RPMI 1640 supplemented with 10% FCS, and a further incubation at 37°C for 20 min. Transfection efficiency and Annexin A1 protein knockdown was assessed 24 and 48 h postpermeabilization by flow cytometric analysis and Western blotting analysis.

2.9 Growth inhibition assay

Cell growth inhibition was performed with CellTiter 96 AQueous One Solution Cell Proliferation Assay (Promega, Madison, USA) according to manufacturer's suggestions. Briefly, after siRNA transfection, cells were seeded onto 96-well plates at a density of 3×10^4 (MM1.S) or 6×10^3 (RPMI8226) cells *per* well and were cultured for 48 h with varying concentrations of dexamethasone (0–10 μM). At the end of the incubation, 20 μL of CellTiter 96 AQueous One solution was added to each well, and the plate was incubated for 1–4 h. The plates were read at 565 nm with 630 nm as a reference using a Model E1 310 Autoplate reader (Bio-Tek Instruments, Winooski, VT, USA).

3 Results

3.1 Comparative proteomic analysis MM cells

To characterize the alterations in protein expression related to MM, we performed 2-DE analysis and proteomic analysis of cellular protein extracts from MM and NPC. For the nine pair samples, we have performed a total of 18 2-DE experi-

ments. Figure 2 shows a pair of representative 2-D gel images for whole cell proteins extracted from MM and NPC. The proteomic maps of MM and NPC were compared with ImageMaster 2D Platinum software to identify the protein spot variations. Seventy-five differentially expressed proteins that could be visualized with silver staining were excised from the 2-D gels and identified by MALDI-TOF/TOF MS followed by database interpretation. Altogether, 43 nonredundant proteins were identified successfully. Table 1 lists the protein identities, together with their spot numbers, molecular weights, p*I*s, *p*-value and fold differences. The detailed information of all identified proteins was presented in the Supporting Information Table 2. The detailed experimental procedures and MS spectra of all identified proteins have been deposited in the Proteomics Identifications Database (PRIDE) (http://www.ebi.ac.uk/pride) with Accession No. 9241.

3.2 Functional categories and biological interaction networking of identified proteins

To understand the biological relevance of the changes in protein expression in MM, PANTHER classification system was used to classify the 43 identified proteins into different functional groups as summarized in Fig. 3A and Table 1. The PANTHER classification system revealed that the proteins can be classified into 16 groups according to their functional properties (Fig. 3A).

Bioinformatic analysis using Pathway Studio software enabled the characterization of biological association networks related to these differentially expressed proteins. The proteins that could be networked were linked by various relationships such as protein interactions, modifications and regulation of expression. These relationships are color coded, and the legends are provided next to the map. A website has been created to host the network (http://life-health.jnu.edu.cn/pathway/pathway.html). The website contains hyperlinks through which the information on the proteins and the nature of their interactions with each other are provided. This website should be useful for formulating testable hypotheses to understand the function of potential diagnostic markers and therapeutic targets of MM. By this approach, we identified some functional groups that may be altered in MM. These include production of energy, calcium regulatory protein, oxidoreductase, *etc.* Several proteins remained orphans because there is insufficient information in the database to link them to other proteins in the network.

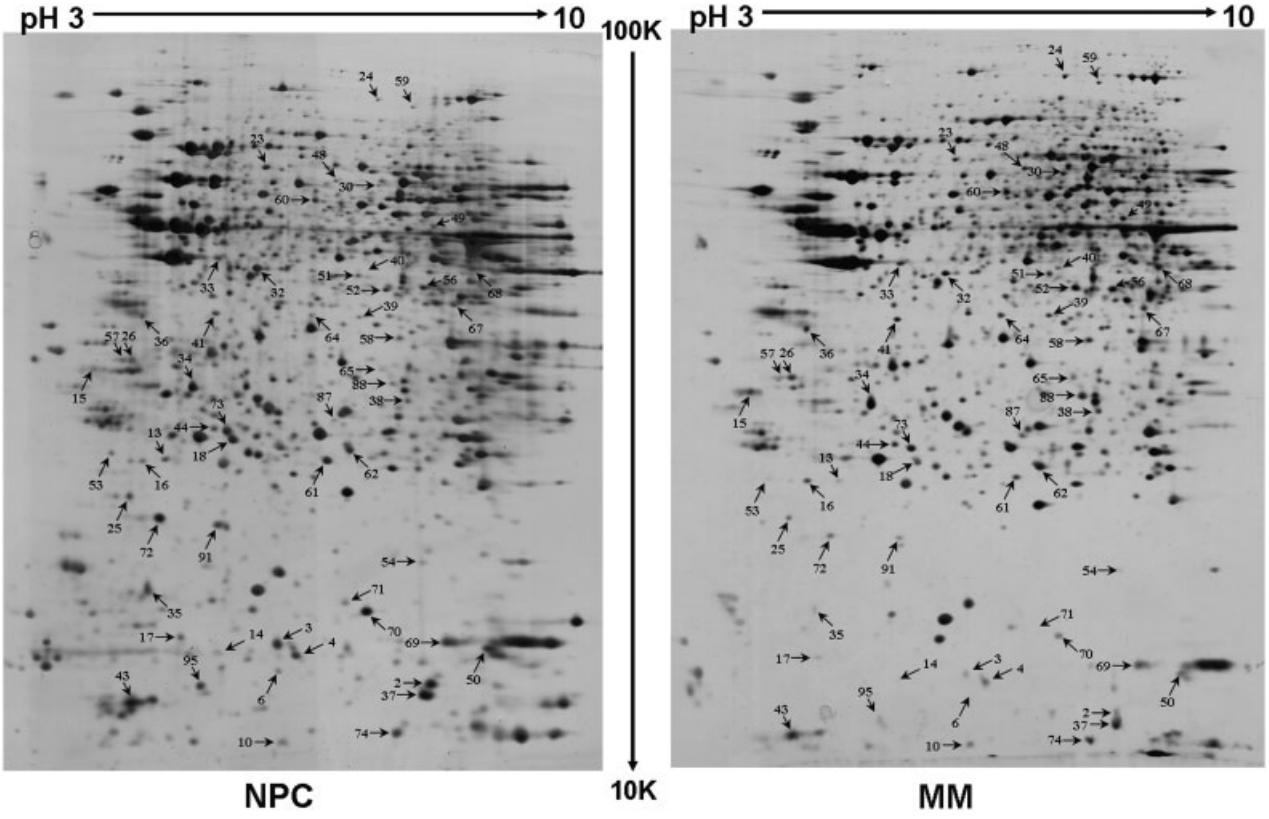

Figure 2. 2-D gel maps of protein expression in MM and NPC. Arrows indicate the changed proteins that were successfully identified. Proteins from the MM or NPCs were extracted and separated on a pH 3–10 NL IPG strip, followed by SDS-PAGE. After staining and image analysis, the spots were analyzed by MALDI-TOF/TOF-MS instrument. The identified proteins, as labeled by number on the gel, are listed in Table 1. Results were from one representative experiment out of nine.

Table 1. Summary of the identified proteins and statistical differences and *p*-values for the comparison between normal and MM cells

Spot no.[a)]	Protein full name[b)]	Accession no.[c)]	Protein MW	Protein p*I*	Protein Score[d)]	MM/NPC[e)]	*p*-value
Cell adhesion molecule							
24	Isoform 2 of vinculin	IPI00307162	123721.8	5.5	306	4.41	0.0021
59	Isoform 2 of vinculin	IPI00307162	123721.8	5.5	512	2.17	0.0043
69	Uncharacterized protein CLC	IPI00873179	16513.3	7.03	89	−2.05	7.12E-05
Chaperone							
41	Activator of 90 kDa heat shock Protein ATPase homolog 1	IPI00030706	38250.2	5.41	97	2.84	1.12E-04
64	AH receptor-interacting protein	IPI00010460	37640.1	6.09	208	2.13	0.0005
Cytoskeletal protein							
25	Translationally-controlled Tumor protein	IPI00550900	19582.6	4.84	173	−3.85	0.0008
35	16 kDa protein	IPI00796881	16266.2	6.29	189	−3.16	2.10E-05
44	CDNA FLJ43573 FIS, Highly similar to actin	IPI00794523	28193	5.2	498	2.69	0.0045
48	Uncharacterized protein WDR1	IPI00873622	66137.9	6.17	138	2.48	0.0225
50	Profilin-1	IPI00216691	15044.6	8.44	282	−2.46	0.0097
60	Coronin-1a	IPI00010133	50993.8	6.25	91	2.16	0.0032
67	Isoform 2 of LIM and SH3 Domain protein 1	IPI00386803	35990.7	8.92	137	2.07	0.0054
88	Isoform 1 of LIM and SH3 Domain protein 1	IPI00000861	29698.2	6.61	316	21.22	4.10E-05
Defense immunity protein							
15	Complement component 1 Q Subcomponent-binding protein	IPI00014230	31342.6	4.74	106	6.24	0.0065
Hydrolase							
30	Protein-arginine deiminase type-4	IPI00008307	74047.4	6.15	182	3.53	0.0082
Isomerase							
65	Isoform 1 of triosephosphate Isomerase	IPI00465028	30771.7	5.65	464	2.12	3.41E-05
70	Peptidyl-prolyl *cis-trans* Isomerase a	IPI00419585	18000.9	7.68	179	−2.05	0.0115
71	Peptidyl-prolyl *cis-trans* Isomerase a	IPI00419585	18000.9	7.68	323	−2.05	0.0091
Kinase							
51	Isoform M2 OFpyruvate kinase Isozymes M1/M2	IPI00479186	57900	7.96	489	2.44	0.0056
56	Isoform M2 of pyruvate kinase Isozymes M1/M2	IPI00479186	57900	7.96	354	2.24	0.0022
91	Cytidine monophosphate (UMP-CMP) Kinase 1, cytosolic	IPI00514929	18966.8	9.06	241	−14.21	0.0063
Ligase							
33	Isoform 2 of succinyl-coA Ligase [ADP-forming] subunit beta	IPI00217232	48009	6.63	233	3.24	4.12E-05

Table 1. Continued

Spot no.[a)]	Protein full name[b)]	Accession no.[c)]	Protein MW	Protein p*I*	Protein Score[d)]	MM/NPC[e)]	*p*-value
Nucleic acid binding							
36	40S ribosomal protein SA	IPI00553164	32833.4	4.79	469	3.07	0.0007
43	Enhancer of rudimentary homolog	IPI00029631	12251	5.63	63	−2.71	0.0027
53	Eukaryotic translation Initiation factor 3 subunit K	IPI00033143	25043.4	4.81	71	−2.31	0.0177
74	12 kDa protein	IPI00793330	12244.6	5.85	192	−2.03	0.0081
Oxidoreductase							
17	Cytochrome c oxidase subunit 5a	IPI00025086	16763.7	6.3	62	−5.95	0.0016
40	Glutamate dehydrogenase 1	IPI00016801	61359.2	7.66	330	2.86	0.0015
62	Glutathione peroxidase 1 isoform 1	IPI00293975	22027.2	6.15	195	2.13	0.0003
72	Nadh dehydrogenase [ubiquinone] Flavoprotein 2	IPI00291328	27374	8.22	142	−2.04	0.0092
73	L-lactate dehydrogenase B chain	IPI00219217	36615.1	5.71	417	−2.03	0.0085
87	Isoform 1 of isocitrate Dehydrogenase [NAD] subunit alpha	IPI00030702	39566.1	6.47	258	11.41	3.17E-05
Phosphatase							
61	Acid phosphatase 1 isoform D	IPI00759646	12222.1	7.63	264	−2.13	0.0048
Protease							
13	Ubiquitin carboxyl-terminal Hydrolase isozyme L1	IPI00018352	24808.5	5.33	152	−7.20	0.0007
18	Ubiquitin carboxyl-terminal Hydrolase isozyme L1	IPI00018352	24808.5	5.33	59	−5.80	0.0311
26	Proteasome subunit alpha type-5	IPI00291922	26394.2	4.74	274	3.69	0.0002
34	Proteasome activator subunit 2	IPI00746205	27384.3	5.54	351	3.19	0.0057
38	Proteasome subunit beta type-10	IPI00027933	28918.1	7.7	237	2.88	0.0028
57	Proteasome subunit alpha type-5	IPI00291922	26394.2	4.74	183	2.23	0.0109
Select calcium binding protein							
2	Protein S100-A8	IPI00007047	10827.7	6.51	232	−27.10	0.0024
3	Protein S100-A9	IPI00027462	13233.5	5.71	384	−18.49	5.25E-06
4	Protein S100-A9	IPI00027462	13233.5	5.71	406	−16.73	0.0357
6	Protein S100-A9	IPI00027462	13233.5	5.71	316	−15.65	0.0029
10	Protein S100-A12	IPI00218131	10568.5	5.83	231	−9.29	0.0028
14	Protein S100-A9	IPI00027462	13233.5	5.71	345	−6.90	0.0105
37	Protein S100-A8	IPI00007047	10827.7	6.51	242	−2.89	0.0066
49	Annexin A11	IPI00414320	54355.1	7.53	290	2.47	0.0042
58	Annexin A1	IPI00218918	38690	6.57	342	2.20	0.0108
95	Protein S100-A9	IPI00027462	13233.5	5.71	365	−12.34	0.0002
Select regulatory molecule							
16	Rho GDP-dissociation inhibitor 1	IPI00003815	23192.7	5.02	351	6.03	0.0001
32	Leukocyte elastase inhibitor	IPI00027444	42714.7	5.9	538	−3.27	0.0025
54	Isoform 2 of cell division Control protein 42 homolog	IPI00016786	21245	6.15	278	−2.30	0.0253
68	Septin	IPI00871851	42657.9	6.38	459	2.07	0.0009

Table 1. Continued

Spot no.[a)]	Protein full name[b)]	Accession no.[c)]	Protein MW	Protein p*I*	Protein Score[d)]	MM/NPC[e)]	*p*-value
Transfer carrier protein							
23	Isoform 1 of serum albumin	IPI00745872	69321.5	5.92	234	−4.43	0.0037
Transferase							
39	Dihydrolipoyllysine-residue Succinyltransferase component Of 2-oxoglutarate Dehydrogenase complex	IPI00420108	48609.4	9.01	185	2.87	2.48E-06
52	Lipoamide acyltransferase Component of branched-chain alpha Keto acid dehydrogenase complex	IPI00003944	53452.9	8.71	64	2.43	0.00117

a) Spot no.: the spot identity on the 2-DE gel designated by the ImageMaster.
b) Protein description in the IPI_HUMAN database.
c) Accession number in the IPI_HUMAN database.
d) Score is $-10*\mathrm{Log}(p)$, where p is the probability that the observed match is a random event; it is based on NCBInr database using the MASCOT searching program as MALDI-TOF data.
e) The ratio of mean normalized values for the corresponding protein spot in MM cells to NPCs. Positive value: up regulation in MM cells; negative value: down regulation in MM cells.

3.3 Validation of differentially expressed proteins in MM

To verify the differential expression of proteins in the MM, we used western blot analysis to examine the expression of a selected panel of proteins, including profilin-1, glutathione peroxidase 1, annexin A1, proteasome subunit alpha type-5 (PSMA5), proteasome activator subunit 2 (PSME2) and proteasome subunit beta type-10 (PSMB10). The Western blotting results showed the same pattern of expression as obtained from 2-DE analysis. That is, profilin-1 expression was significantly decreased, while annexin A1, glutathione peroxidase 1 and all three proteasome subunits expression were significantly increased in MM (Fig. 4).

3.4 Annexin A1 knock-down potentiates dexamethasone-induced lethality of dexamethasone-sensitive and dexamethasone-resistant human MM cells

To investigate the effect of annexin A1 inhibition in MM cells and whether annexin A1 has a role in dexamethasone-induced apoptosis, we used RNAi to reduce cellular annexin A1 levels and examine the effect of annexin A1 knock down. The effect of the annexin A1 siRNA in silencing the annexin A1 gene in myeloma cells was examined by directly measuring changes in annexin A1 protein levels. As shown in Fig. 5A, transfection of cells with the annexin A1 siRNA resulted in a significant decrease in the level of annexin A1 protein, whereas mock transfection with a random siRNA had no such effect. This effect was specific because the annexin A1 siRNA did not change the levels of tubulin protein (Fig. 5A).

To determine whether annexin A1 knock down affects viability of MM cells, we first studied MM1.S cells that are sensitive to dexamethasone-induced killing. MM1.S cells were transfected with annexin A1 siRNA for 48 h and then monitored for viability. Under these experimental conditions, annexin A1 knock down decreased viability by ~7% (Fig. 5B). MM1.S cells also responded to 10^{-8} to 10^{-5} mol/L dexamethasone alone with loss of viability. Moreover, annexin A1 knock down combined with dexamethasone resulted in a greater than additive loss of MM1.S cell viability compared with that found with either treatment alone, whereas mock transfection with a random siRNA had no such effect (Fig. 5B). Similar studies were performed on the dexamethasone-resistant RPMI8226 cells. RPMI8226 cells were transfected with annexin A1 siRNA for 48 h and the cell viability was decreased by ~9%. For both cell lines, statistical analysis indicated that the percentage of viable cells in ANXA1 siRNA-transfected cells was significantly lower than that of a random siRNA-transfected group ($p<0.05$). In contrast to MM1.S cells, treatment of the RPMI8226 cells with dexamethasone

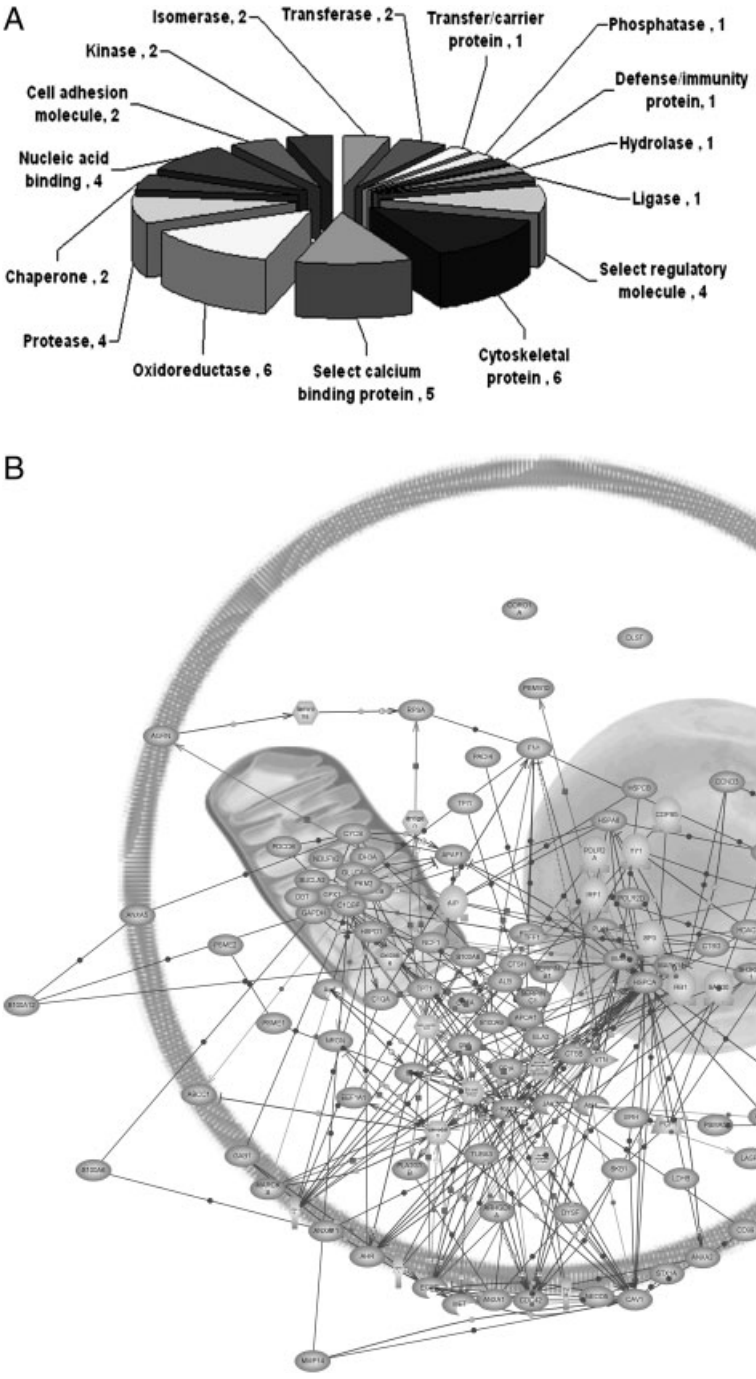

Figure 3. Bioinformatics analysis of the differentially expressed proteins. (A) Pie chart representations of the distribution of identified proteins according to their molecular functions. Categorizations were based on information provided by the online resource PANTHER classification system. Some proteins were annotated manually based on literature searches and closely related homologues. (B) Pathway mapping of altered protein expression using Pathway Studio. Proteins identified in Table 1 were imported into PathwayAssist, and an interaction map was generated. Shown are proteins that either bound directly to another identified protein or to another identified protein *via* one other protein. Each node represents either a protein entity or a control mechanism of the interaction. The legend of the interaction network is summarized on the right of the figure. The biological network can be accessed *via* (http://life-health.j-nu.edu.cn/pathway/pathway.html).

alone at concentrations of 10^{-8} to 10^{-5} mol/L had little if any effect on viability (Fig. 5C). However, the combination of annexin A1 knock down and dexamethasone resulted in cytotoxicity that was greater than that achieved with either treatment alone (Fig. 5C). These findings indicate that annexin A1 knock down modestly induces lethality alone and potentiates the effects of dexamethasone on both dexamethasone-sensitive and dexamethasone-resistant MM cells.

4 Discussion

As in most cancers, tumorigenesis of MM involves multiple steps and factors [1]. The large-scale RNA-expression analysis has generated extensive datasets relating to tumorigenesis and classification of MM. Although the transcriptome analysis of MM was instructive, it is clear that the molecular mechanisms involved in MM formation cannot be understood from the analysis of the transcriptome

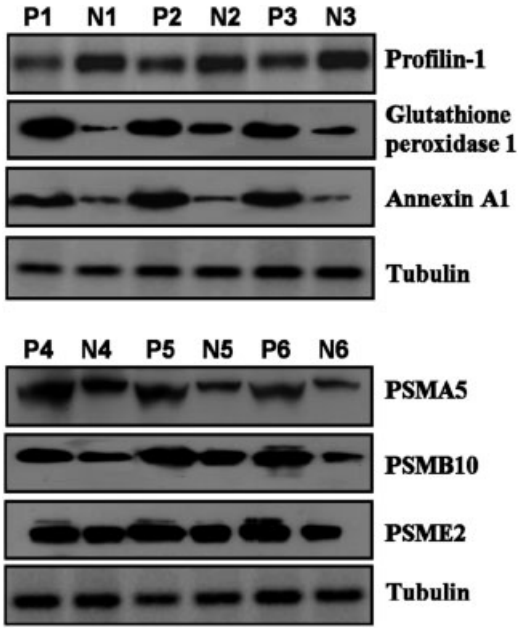

Figure 4. Western blot images for six proteins and internal control protein tubulin. Western blotting shows changes in the expression levels of profilin-1, glutathione peroxidase 1, annexin A1, PSMA5, PSME2 and PSMB10 in MM (P) and NPC (N).

alone. Systematic comparison of changes in the protein composition in MM and NPCs should provide clues for wide studies of mechanisms that underlie the formation and physiopathology of MM.

Results of comparative proteomic studies of human MM, to our knowledge, are not yet available for the scientific community. This study is the first to employ proteomic technique to globally search for the dysregulated proteins in MM. In this experiment, we carried out comparative proteome analysis of MM and NPC with the aim to identify clusters of proteins (and pathways) that showed differential expression. A total of 43 differentially expressed proteins were identified by MS, and differential expression levels of six identified proteins (profilin-1, glutathione peroxidase 1, annexin A1, PSMA5, PSME2, and PSMB10) in NPCs and MM were confirmed by Western blotting, suggesting that the proteins identified by proteomic approach are actually differential expression proteins. Importantly, some of the identified proteins have been previously seen in global gene expression analyses [15].

The cytoskeletal proteins represented the largest group in all identified proteins. The cytoskeleton is a highly complex and dynamic system comprising structural proteins forming polymers and several associated proteins with regulatory functions. In addition to their well-known structural function, cytoskeletal proteins play important roles in cell mobility and migration, immunological synapse formation, and apoptosis. Tumor-associated changes in the cytoskeleton are well documented and even used in cancer diagnostics [16]. For example, profilin-1, a ubiquitously

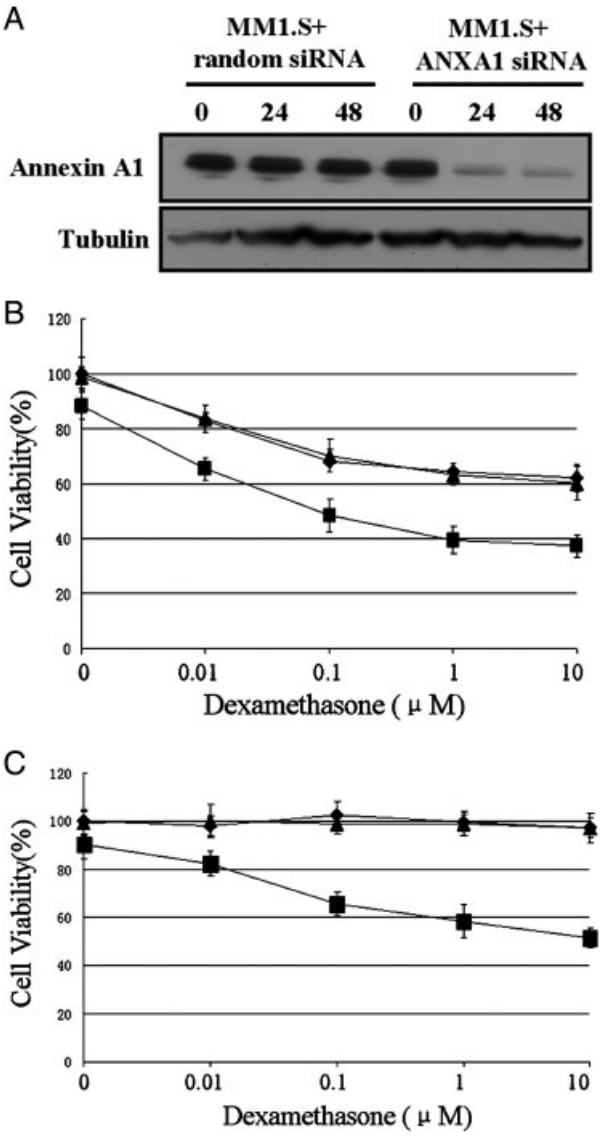

Figure 5. Lethality of MM cells induced by ANXA1 knock down alone and in combination with dexamethasone. (A) The knock down of ANXA1 in MM cells was confirmed by Western blotting analysis. (B) MM1.S cells with mock transfection(♦) or with random siRNA transfection(▲) or ANXA1 knock down (■) were treated with the indicated concentrations of dexamethasone for 48 h. The number (mean±SD of three replicates) of viable cells was determined by MTT assay. (C) RPMI8226 cells with mock transfection (♦) or with random siRNA transfection (▲) or with ANXA1 knock down (■) were treated with the indicated concentrations of dexamethasone for 48 h. The number (mean±SD of three replicates) of viable cells was determined by MTT assay.

expressed G-actin-binding protein, is found to be expressed at a significantly low level in MM cells and also in human breast cancer tissue and a variety of breast carcinoma cell lines [17], pancreatic [18] and hepatic [19] carcinoma cells compared to their normal counterparts. These interesting

observations appear to suggest that loss of profilin-1 expression may have a general relevance in cancer progression. Profilin-1 overexpressing breast cancer cells failed to form tumors when xenografted subcutaneously in nude mice, which suggested that profilin-1 could also be a tumor-suppressor protein [20]. Profilin-1 also has been implicated in a wide range of cellular activities including proliferation, migration, endocytosis, mRNA splicing, and gene transcription [21]. A large number of pathogen-based model studies have implied profilin-1's function in actin-based protrusion during cell migration [22]. Given these findings, it is thus not clear why profilin-1 expression is significantly downregulated in MM cells and many other different types of cancer cells. We postulated that profilin-1 is a negative regulator of MM aggressiveness and perturbing profilin-1 could be a good molecular strategy to limit the aggressiveness of MM cells. Related to this postulate, we are investigating how loss of profilin-1 expression affects the motility of MM cells and the effects of overexpression of either functional or ligand-binding deficient mutants of profilin-1 on MM cell motility.

As shown in Fig. 4, three proteasome subunits, *e.g.* proteasome subunit alpha type-5 (PSMA5), proteasome activator subunit 2 (PSME2), and proteasome subunit beta type-10 (PSMB10), were upregulated in MM cells. The proteasome plays a pivotal role in the degradation of short-lived regulatory proteins, which are components of cell cycle regulation, cell surface receptors, ion channels modulation, and antigen presentation. It is believed that once the disposal system fails to work, the substances, such as regulatory molecules p53, NFκB, and Bax that promote apoptosis, may accumulate to a high level harmful to the cell [23, 24]. Overexpression of proteasomal proteins was frequently associated with leukemia [25], renal carcinomas [26], and breast cancers [27]. Multiple studies show that proteasome inhibitors are more cytotoxic to proliferating malignant cells than to quiescent normal cells [28, 29]. Our findings suggest that the MM cells have altered proteasomal proteins and higher dependency on the proteasomal degradation processes. The results from this study would provide new insights into the formation of MM and mechanisms of proteasome inhibitor PS-341 (bortezomib) on MM.

The expression of six oxidoreductases was increased in MM samples: a value that testifies the relevance of this class of proteins in the pathogenesis of MM. This class includes cytochrome c oxidase, glutathione peroxidase 1 (GPX1), and four kinds of dehydrogenases. It has been reported that oxidative stress mediates various cellular responses, and that the control of reduction/oxidation (redox) is fundamental in maintaining the homeostasis of the whole organism [30]. Among these enzymes, glutathione peroxidase 1 plays an important role in the detoxification of H_2O_2, antioxidant defense of the vascular wall, and neural cells in response to oxidative stress, and it is one of the most important antioxidant enzymes in humans [31, 32]. It is now well appreciated that MM is characterized by enhanced production of reactive metabolites of oxygen and nitrogen species [33]. Consistent with our findings, previous studies showed that antioxidant enzymes activity, including GPX1, increased in MM patients and decreased significantly after vincristine–adriamycin–dexamethasone therapy [34]. Therefore, we speculate that upregulation of GPX1 may play significant roles in pathogenesis of MM and could be used as the potential drug targets.

Another large functionally related group contained some calcium ion-binding proteins belonging to annexin and S100 families. Three members of the S100 family were significantly downregulated in MM and two members of the annexin family were upregulated. Notably, previously published gene expression profiling studies also showed the downregulation of S100A9 and S100A12 genes at mRNA level in MM cells [15]. Further experiments will be performed to elucidate whether the downregulation of S100 proteins in MM cells is functionally important to benefit carcinogenesis of MM. On the 2-D gel, S100A9 proteins are represented by multiple spots. The multiple spots may result from phosphorylation, glycosylation, or other PTMs. Each of these isoforms could play a specific cellular role, which waits for further functional investigations.

Interestingly, annexin A1 and annexin A11 were upregulated in MM cells. Both proteins belong to the same subgroup of the annexin family. Annexins are calcium- and phospholipid-binding proteins forming an evolutionary conserved multigene family, with members of the family being widely expressed in mammals [35]. The dysregulation of annexin family members have been reported in numerous cancers and influence the patterns of cellular behavior, such as cell proliferation, motility, invasiveness, and signalling pathways, suggesting that annexins may play important roles in tumor development and progression and serve as potential biomarkers for the diagnosis and treatment of cancer [36]. Annexin A1, a 37-kDa protein, is claimed to participate in cell transformation as well as in inflammation, signal transduction, keratinocyte differentiation, apoptosis, and gene expression modulation [37–39]. The relationship between annexin A1 and the neoplastic process may be derived from the fact that it is a substrate of EGFR and other kinases involved in tumor development [40]. ANXA1 has been shown to be upregulated in pancreatic carcinoma [41], hairy cell leukemia [42], and skin tumors [43]. In this study, we found that annexin A1 was upregulated in MM by proteomic profile analysis, which was further validated by the results of Western blot. Then, we tested the effects of annexin A1 knock down on the growth of MM cells and our results indicated that annexin A1 knock down modestly induces lethality of MM cells. Based on previous reports, ANXA1 influences dexamethasome-induced changes in cell proliferation [44] and dexamethasome confers the resistance of human leukemic U937 cells to tumor necrosis factor-induced apoptosis by upregulating intracellular levels of annexin A1 and by facilitating a

negative-feedback loop, which is activated upon stimulation with tumor necrosis factor. High constitutive levels of annexin A1 in leukemic blasts may protect them against immune-mediated killing [45]. These reports prompted us to investigate whether annexin A1 has a role in dexamethasome-induced changes in MM. Our results demonstrate that annexin A1 knock down potentiates dexamethasone-induced killing of both dexamethasone-sensitive MM1.S and dexamethasone-resistant RPMI8226 MM cells. Knock down of annexin A1 appeared to modestly induce lethality in MM cells, suggesting a possibility that upregulation of annexin A1 may be part of the oncogene addiction machinery that MM cells rely on for survival. Together with the fact that RNAi-based annexin A1 knock-down potentiates the effects of dexamethasone on both dexamethasone-sensitive and dexamethasone-resistant MM cells, this notion implicates an attractive opportunity for therapeutic development by inhibiting annexin A1. In addition, because annexin A1 is upregulated in other cancers, such as pancreatic carcinoma and hairy cell leukemia, development of small-molecule inhibitors of annexin A1 may find broad therapeutic applications.

The proteome is a highly dynamic entity, being constantly altered during the cell lifetime. Additionally, changes in protein levels do not result exclusively from up- or downregulation of their respective gene expression. It could result from PTMs and different processing and/or turnover rates. Therefore, the independent validation of each protein identified here as a contributor to MM pathophysiology will be necessary. Once validated, MM biomarkers could also be potential targets for the development of new MM therapies. Although more studies are needed, the proteins identified here could potentially be biomarkers and/or therapeutic targets for MM. In this study, proteomics techniques and sampling scheme proved effective and promising to identify proteins important to pathogenesis of MM. Furthermore, similar to investigations in leukemia [46, 47], protein expression profiling is anticipated to result in the identification of distinct and prognostically relevant clinical subgroups of MM.

This work was supported by the Open Research Fund Program of the State Key Laboratory of Virology of China (Grant 2009003), Talents Start-up Foundation of Jinan University (Grant 51207040) and the Program for New Century Excellent Talents in University (NCET-07-0376)

The authors have declared no conflict of interest.

5 References

[1] Mitsiades, C. S., Mitsiades, N. S., Munshi, N. C., Anderson, K. C., Focus on multiple myeloma. *Cancer Cell* 2004, *6*, 439–444.

[2] Jemal, A., Siegel, R., Ward, E., Hao, Y. *et al.,* Cancer statistics. *CA Cancer J. Clin.* 2008, *58*, 71–96.

[3] Yang, L., Parkin, D. M., Ferlay, J., Li, L., Chen, Y., Estimates of cancer incidence in China for 2000 and projections for 2005. *Cancer Epidemiol. Biomarkers Prev.* 2005, *14*, 243–250.

[4] Hideshima, T., Mitsiades, C., Tonon, G., Richardson, P. G., Anderson, K. C., Understanding multiple myeloma pathogenesis in the bone marrow to identify new therapeutic targets. *Nat. Rev. Cancer* 2007, *7*, 585–598.

[5] Tassone, P., Tagliaferri, P., Rossi, M., Gaspari, M. *et al.,* Genetics and molecular profiling of multiple myeloma, novel tools for clinical management? *Eur. J. Cancer* 2006, *42*, 1530–1538.

[6] Zhan, F., Tian, E., Bumm, K., Smith, R. *et al.,* Gene expression profiling of human plasma cell differentiation and classification of multiple myeloma based on similarities to distinct stages of late-stage B-cell development. *Blood* 2003, *101*, 1128–1140.

[7] Shi, T., Dong, F., Liou, L. S., Duan, Z. H. *et al.,* Differential protein profiling in renal-cell carcinoma. *Mol. Carcinog.* 2004, *40*, 47–61.

[8] Mitsiades, C. S., Mitsiades, N., Treon, S. P., Anderson, K. C., Proteomic analyses in Waldenstrom's macroglobulinemia and other plasma cell dyscrasias. *Semin. Oncol.* 2003, *30*, 156–160.

[9] Ge, F., Lu, X. P., Zeng, H. L., He, Q. Y. *et al.*, Proteomic and functional analyses reveal a dual molecular mechanism underlying arsenic-induced apoptosis in human multiple myeloma cells. *J. Proteome Res.* 2009, *8*, 3006–3019.

[10] Rees-Unwin, K. S., Craven, R. A., Davenport, E., Hanrahan, S. *et al.,* Proteomic evaluation of pathways associated with dexamethasone-mediated apoptosis and resistance in multiple myeloma. *Br. J. Haematol.* 2007, *139*, 559–567.

[11] Jennings, C. D., Foon, K. A., Recent advances in flow cytometry, application to the diagnosis of hematologic malignancy. *Blood* 1997, *90*, 2863–2892.

[12] Mi, H., Guo, N., Kejariwal, A., Thomas, P. D., PANTHER version 6, Protein sequence and function evolution data with expanded representation of biological pathways. *Nucleic Acids Res.* 2007, *35*, D247–D252.

[13] Nikitin, A., Egorov, S., Daraselia, N., Mazo, I., Pathway studiothe analysis and navigation of molecular networks. *Bioinformatics* 2003, *19*, 2155–2157.

[14] Brito, J. L., Davies, F. E., Gonzalez, D., Morgan, G. J., Streptolysin-O reversible permeabilisation is an effective method to transfect siRNAs into myeloma cells. *J. Immunol. Methods* 2008, *333*, 147–155.

[15] Zhan, F., Hardin, J., Kordsmeier, B., Bumm, K. *et al.,* Global gene expression profiling of multiple myeloma, monoclonal gammopathy of undetermined significance, and normal bone marrow plasma cells. *Blood* 2002, *99*, 1745–1757.

[16] Ditzel, H. J., Strik, M. C., Larsen, M. K., Willis, A. C. *et al.,* Cancer-associated cleavage of cytokeratin 8/18 heterotypic complexes exposes a neoepitope in human adenocarcinomas. *J. Biol. Chem.* 2002, *277*, 21712–21722.

[17] Janke, J., Schluter, K., Jandrig, B., Theile, M. *et al.,* Suppression of tumorigeniciy in breast cancer cells by the microfilament protein profilin 1. *J. Exp. Med.* 2000, *191*, 1675–1685.

[18] Gronborg, M., Kristiansen, T. Z., Iwahori, A., Chang, R. *et al.,* Biomarker discovery from pancreatic cancer secretome using a differential proteomic approach. *Mol. Cell. Proteomics* 2006, *5*, 157–171.

[19] Wu, N., Zhang, W., Yang, Y., Liang, Y. L. *et al.,* Profilin 1 obtained by proteomic analysis in all-trans retinoic acid-treated hepatocarcinoma cell lines is involved in inhibition of cell proliferation and migration. *Proteomics* 2006, *6*, 6095–6106.

[20] Wittenmayer, N., Jandrig, B., Rothkegel, M., Schlüter, K. *et al.,* Tumor suppressor activity of profilin requires a functional actin binding site. *Mol. Biol. Cell* 2004, *15*, 1600–1608.

[21] Witke, W., The role of profilin complexes in cell motility and other cellular processes. *Trends Cell Biol.* 2004, *14*, 461–469.

[22] Grenklo, S., Geese, M., Lindberg, U., Wehland, J. *et al.,* A crucial role for profilin-actin in the intracellular motility of listeria monocytogenes. *EMBO Rep.* 2003, *4*, 523–529.

[23] Schwartz, A. L., The ubiquitin-proteasome pathway and pathogenesis of human disease. *Annu. Rev. Med.* 1999, *50*, 57–74.

[24] Hernandez, F., Diaz-Hernandez, M., Avila, J., Lucas, J. J., Testing the ubiquitin-proteasome hypothesis of neurodegeneration *in vivo*. *Trends Neurosci.* 2004, *27*, 66–69.

[25] Kumatori, A., Tanaka, K., Inamura, N., Sone, S. *et al.,* Abnormally high expression of proteasomes in human leukemic cells. *Proc. Natl. Acad. Sci. USA* 1990, *87*, 7071–7075.

[26] Kanayama, H., Tanaka, K., Aki, M., Kagawa, S. *et al.,* Changes in expressions of proteasome and ubiquitin genes in human renal cancer cells. *Cancer Res.* 1991, *51*, 6677–6685.

[27] Choi, Y. H., Proteasome-mediated degradation of BRCA1 protein in MCF-7 human breast cancer cells. *Int. J. Oncol.* 2001, *19*, 687–693.

[28] Bogner, C., Schneller, F., Hipp, S., Ringshausen, I. *et al.,* Cycling B-CLL cells are highly susceptible to inhibition of the proteasome, involvement of p27, early D-type cyclins, Bax, and caspase-dependent and -independent pathways. *Exp. Hematol.* 2003, *31*, 218–225.

[29] Schenkein, D., Proteasome inhibitors in the treatment of B-cell malignancies. *Clin. Lymphoma* 2002, *3*, 49–55.

[30] Nishinaka, Y., Nakamura, H., Masutani, H., Yodoi, J., *Archiv. Immunol. Ther. Exper.* 2001, *49*, 285–292.

[31] Crack, P. J., Taylor, J. M., Flentjar, N. J., de Haan, J. *et al.,* Increased infarct size and exacerbated apoptosis in the glutathione peroxidase-1 (GPx-1) knockout mouse brain in response to ischemia/reperfusion injury. *J. Neurochem.* 2001, *78*, 1389–1399.

[32] Hussain, S. P., Amstad, P., He, P., Robles, A. *et al.,* p53-induced upregulation of MnSOD and GPx but not catalase increases oxidative stress and apoptosis. *Cancer Res.* 2004, *64*, 2350–2356.

[33] Zima, T., Spicka, S., Crkovska, J., Platenik, J. *et al.,* Antioxidant enzymes and lipid peroxidation in patients with multiple myeloma. *Neoplasma* 1996, *43*, 69–73.

[34] Kuku, I., Aydogdu, I., Bayraktar, N., Kaya, E. *et al.,* Oxidant/antioxidant parameters and their relationship with medical treatment in multiple myeloma. *Cell Biochem. Funct.* 2005, *23*, 47–50.

[35] Gerke, V., Moss, S. E., Annexins, from structure to function. *Physiol. Rev.* 2002, *82*, 331–371.

[36] Rescher, U., Gerke, V., Annexins—unique membrane binding proteins with diverse functions. *J. Cell Sci.* 2004, *117*, 2631–2639.

[37] Alldridge, L. C., Harris, H. J., Plevin, R., Hannon, R., Bryant, C. E., The annexin protein lipocortin 1 regulates the MAPKERK pathway. *J. Biol. Chem.* 1999, *274*, 37620–37628.

[38] Solito, E., Kamal, A., Russo-Marie, F., Buckingham, J. C. *et al.,* A novel calcium-dependent proapoptotic effect of annexin 1 on human neutrophils. *FASEB J.* 2003, *17*, 1544–1546.

[39] Rodrigues-Lisoni, F. C., Mehet, D. K., Peitl, P., John, C. D. *et al., In vitro* and *in vivo* studies on CCR10 regulation by Annexin A1. *FEBS Lett.* 2006, *580*, 1431–1438.

[40] Gerke, V., Moss, S. E., Annexins, from structure to function. *Physiol. Rev.* 2002, *82*, 331–371.

[41] Bai, X. F., Ni, X. G., Zhao, P., Liu, S. M. *et al.,* Overexpression of annexin 1 in pancreatic cancer and its clinical significance. *World J. Gastroenterol.* 2004, *10*, 1466–1470.

[42] Falini, B., Tiacci, E., Liso, A., Basso, K. *et al.,* Simple diagnostic assay for hairy cell leukaemia by immunocytochemical detection of annexin A1 (ANXA1). *Lancet* 2004, *363*, 1869–1870.

[43] Hummerich, L., Muller, R., Hess, J., Kokocinski, F. *et al.,* Identification of novel tumour-associated genes differentially expressed in the process of squamous cell cancer development. *Oncogene* 2006, *25*, 111–121.

[44] Croxtall, J. D., Flower, R. J., Lipocortin-1 mediates dexamethasone-induced growth arrest of the A549 lung adenocarcinoma cell line. *Proc. Natl. Acad. Sci. USA* 1992, *89*, 3571–3575.

[45] Wu, Y. L., Jiang, X. R., Lillington, D. M., Newland, A. C., Kelsey, S. M., Upregulation of lipocortin 1 inhibits tumour necrosis factor-induced apoptosis in human leukaemic cells, a possible mechanism of resistance to immune surveillance. *Br. J. Haematol.* 2000, *111*, 807–816.

[46] Kornblau, S. M., Tibes, R., Qiu, Y. H., Chen, W. *et al.,* Functional proteomic profiling of AML predicts response and survival. *Blood* 2009, *113*, 154–164.

[47] Fontana, S., Alessandro, R., Barranca, M., Giordano, M. *et al.,* Comparative proteome profiling and functional analysis of chronic myelogenous leukemia cell lines. *J. Proteome Res.* 2007, *6*, 4330–4342.

